

Catalytic Reduction of Nitrogen Oxides by Propene in the Presence of Oxygen over Cerium Ion-Exchanged Zeolites

III. Effects of Carriers

Chikafumi Yokoyama and Makoto Misono¹

Department of Applied Chemistry, Faculty of Engineering, University of Tokyo, Hongo, Bunkyo-ku, Tokyo 113, Japan

Received August 7, 1995; revised December 28, 1995; accepted January 5, 1996

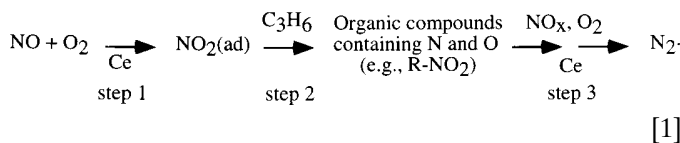
The mechanism of catalytic reduction of NO_x by propene in the presence of oxygen, NO (or NO₂) + C₃H₆ + O₂ reaction, over Ce-supported catalysts was studied, focusing on the relative activities of catalysts and carriers for several relevant reactions. The rate of N₂ formation in the NO + C₃H₆ + O₂ reaction was very much dependent on the kinds of carriers, the rate being in the order of Ce-ZSM-5 > Ce-mordenite ≫ Ce-Y zeolite > Ce/SiO₂. This order was very different from the order observed for the rate of NO + 1/2O₂ → NO₂, that is, Ce-mordenite > Ce-ZSM-5 ≈ Ce-Y zeolite ≈ Ce/SiO₂, although the latter reaction was the initial and indispensable step for the NO + C₃H₆ + O₂ reaction [C. Yokoyama and M. Misono, *J. Catal.* 150, 9 (1994)]. However, the former order was the same as that for the formation of N₂ in NO₂ + C₃H₆ + O₂ reaction over the carriers alone (Na-ZSM-5 > Na-mordenite > Na-Y zeolite ≈ silicalite > SiO₂). It was confirmed that NO + C₃H₆ + O₂ reaction did not proceed on the carriers alone as they had little activity for NO oxidation. These activity orders were reasonably explained by the important role of carriers in the formation of N₂ from the reaction between propene and NO₂, which is the step subsequent to the oxidation of NO to NO₂ in the NO + C₃H₆ + O₂ reaction. The rates of NO₂ + C₃H₆ + O₂ reaction over the carriers (Na-zeolites, silicalite, and silica) were proportional to the amounts of propene adsorbed on the carriers at room temperature. On the other hand, the amount of NO₂ adsorbed was significantly greater and comparable with the Na content. On the basis of these results, it is proposed that the active sites of these carriers for this reaction are Na ions which can adsorb propene in addition to NO₂. Accordingly, it is suggested that the active sites of Ce zeolites are Ce ion exchanged at these active Na sites. © 1996 Academic Press, Inc.

INTRODUCTION

For the abatement of NO_x from the exhaust gases of diesel and lean-burn gasoline engines, catalytic reduction of NO_x by hydrocarbons in excess of oxygen has attracted attention. Since patents (1) and reports of Iwamoto (2) and

Held *et al.* (3) on Cu-zeolites were published, several catalysts such as H-zeolite (4), Al₂O₃ (5), Ga-zeolite (6), Co-zeolite (7), and Cu-silicate (8) have been reported. We have previously found that Ce ion-exchanged zeolites are very active for the reduction of NO by propene and that the activity is enhanced by the addition of alkaline earths to Ce-ZSM-5 or the increase in the level of Ce-doping (9–11).

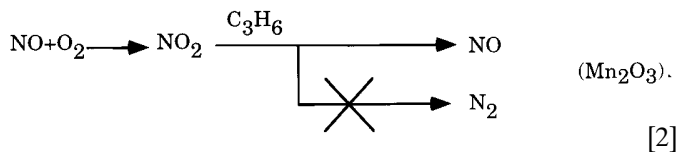
As for the mechanism, it was reported that NO₂ (12, 13) or the partially oxidized hydrocarbons (14) were the intermediate. We proposed a mechanism of NO + C₃H₆ + O₂ reaction over Ce-ZSM-5 as follows (15, 16):



Here, the overall reaction is divided into three steps: NO is oxidized to NO₂ by oxygen on the surface (Ce ion) (step 1), NO₂(ad) or NO₂ in the gas phase reacts rapidly with propene to form organic compounds containing N and/or O (e.g., R-NO₂) (step 2), and these compounds are oxidatively decomposed to N₂ and CO_x (step 3). The doped Ce accelerates the steps 1 and 3. The difference between the $\text{NO} + \text{C}_3\text{H}_6 + \text{O}_2$ and $\text{NO}_2 + \text{C}_3\text{H}_6 + \text{O}_2$ are crucial for catalysts which are not active for the step 1, i.e., the oxidation of NO to NO₂. There have been some reports with regard to steps 2 and 3. Lukyanov *et al.* have suggested that organic nitro compounds are deposited on the catalyst and that these react with NO_x to form an N–N bond leading to release of N₂ (17). Radtke *et al.* reported that HNCO as well as HCN was formed into gas phase in the case of NO + olefins + O₂ reaction over Cu-ZSM-5 (18, 19). We reported the formation of HCN, C₂N₂, and probably HNCO in these reactions (15, 20) and the formation of N₂ from the reaction of adsorbed organic nitro compounds with NO₂ and O₂ (21). Intermediacy of organic nitro and nitrite compounds has been indicated for Pt-SiO₂ (22).

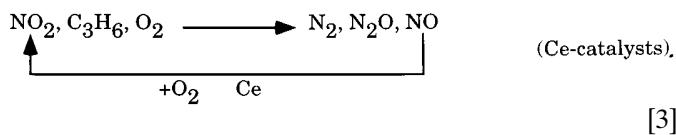
¹ To whom correspondence should be addressed. Fax: 81-3-5802-2949.

On the basis of this mechanism, we have found that a mechanical mixing of Mn_2O_3 or CeO_2 , which has a higher activity for $\text{NO} + 1/2\text{O}_2 \rightarrow \text{NO}_2$, with Ce-ZSM-5 enhances the activity for $\text{NO} + \text{C}_3\text{H}_6 + \text{O}_2$ reaction in the low to medium temperature region (23). However, N_2 was not formed at all for $\text{NO} + \text{C}_3\text{H}_6 + \text{O}_2$ reaction over Mn_2O_3 alone (in the absence of Ce-ZSM-5), although Mn_2O_3 had a high activity for $\text{NO} + 1/2\text{O}_2 \rightarrow \text{NO}_2$, and NO_2 in $\text{NO}_2 + \text{C}_3\text{H}_6 + \text{O}_2$ reaction was all converted to NO , as shown in



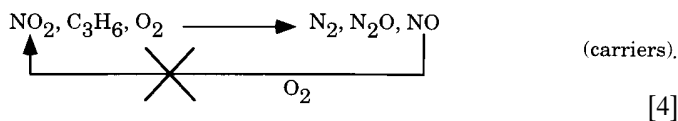
These facts indicate that not only the oxidation of NO to NO_2 but also the subsequent reactions between NO_2 (adsorbed or in the gas phase) and propene are important for N_2 formation (steps 2 and 3, Eq. [1]) in the $\text{NO} + \text{C}_3\text{H}_6 + \text{O}_2$ reaction. In other words, Ce-ZSM-5 appears to possess a "special active site" for the production of N_2 through the reaction between NO_2 and propene. There have been reports (24–26) which indicate a significant influence of carriers in these reactions. However, the influence is still not clear and the "special active site" is worthy to elucidate. In this work, we examined the effects of the carriers on the N_2 formation for $\text{NO} + \text{C}_3\text{H}_6 + \text{O}_2$ reaction, paying particular attention to the reaction between NO_2 and propene.

In the case of $\text{NO}_2 + \text{C}_3\text{H}_6 + \text{O}_2$ reaction, NO_2 was converted not only to N_2 but also to NO . On Ce-supported catalysts, since the oxidation of NO to NO_2 occurs, NO formed in $\text{NO}_2 + \text{C}_3\text{H}_6 + \text{O}_2$ reaction is oxidized to NO_2 again (Eq. [3]). Due to this secondary reaction (oxidation of NO to NO_2), the initial selectivities (see below) for $\text{NO}_2 + \text{C}_3\text{H}_6 + \text{O}_2$ reaction over these catalysts are difficult to determine:



Accordingly, we examined the $\text{NO}_2 + \text{C}_3\text{H}_6 + \text{O}_2$ reaction over carriers alone. Since both $\text{NO} + 1/2\text{O}_2 \rightarrow \text{NO}_2$ and $\text{NO} + \text{C}_3\text{H}_6 + \text{O}_2 \rightarrow \text{N}_2 + \text{CO}_x + \text{H}_2\text{O}$ are very slow on the carriers, NO formed in $\text{NO}_2 + \text{C}_3\text{H}_6 + \text{O}_2$ reaction would stay unchanged (Eq. [4]). Hence, the comparison of rates and selectivities of $\text{NO}_2 + \text{C}_3\text{H}_6 + \text{O}_2$ reaction would be easier in the case of carriers alone. We also examined the adsorptions of propene and NO_2 on the carriers to elucidate the "special active site" for N_2 formation in the reaction between NO_2 and propene. In this work, the discussion is principally based on the relative activities of Ce- and Na-zeolites for $\text{NO} + \text{C}_3\text{H}_6 + \text{O}_2$, $\text{NO}_2 + \text{C}_3\text{H}_6 + \text{O}_2$, and

$\text{NO} + \text{O}_2$ reactions:



EXPERIMENTAL

Catalysts

Na-ZSM-5 ($\text{SiO}_2/\text{Al}_2\text{O}_3 = 23.3$, kindly provided by Tosoh Corporation), Na-mordenite ($\text{SiO}_2/\text{Al}_2\text{O}_3 = 20.1$, JRC-Z-M20), and Na-Y zeolite ($\text{SiO}_2/\text{Al}_2\text{O}_3 = 5.6$, JRC-Z-Y5.6) were prepared as follows in order to obtain complete Na ion-exchange: zeolites were stirred in sodium acetate solution for 24 h, filtered, stirred in deionized water, filtered, washed by deionized water several times, and dried at 373 K for 24 h. Silicalite ($\text{SiO}_2/\text{Al}_2\text{O}_3 = 2100$, Na; 0.01 wt%, provided by Tosoh Corporation) and SiO_2 (Na; 0.0001 wt%, JRC-SIO-4) were used without further treatment. Ce was doped by ion-exchange from the Na-zeolites in aqueous solution of cerium acetate (Ce^{3+}) at room temperature for ZSM-5, mordenite, and Y zeolite. The ion-exchange was carried out twice for ZSM-5 and once for mordenite and Y zeolite. The exchange level was estimated by measuring the amount of Na eluted in the filtrate by means of atomic adsorption spectroscopy. Ce/ SiO_2 was prepared by the impregnation of a cerium acetate solution to SiO_2 , followed by drying at 373 K and calcination in air at 773 K for 4 h. The contents of Ce were 1.1 wt% as Ce (corresponding to ion-exchange level of 19%) for ZSM-5, 4.3 wt% (64%) for mordenite, 9.9 wt% (53%) for Y zeolite, 5 wt% for SiO_2 . Hereafter, ZSM-5, mordenite, Y zeolite, silicalite, and SiO_2 are denoted by Z, M, Y, SL, and SI, respectively. Two kinds of proton exchanged ZSM-5 were prepared by ion-exchange of the Na-ZSM-5 with an ammonium nitrate solution, followed by drying at 373 K and calcination in air at 773 K for 4 h. The ion-exchange levels were 10 and 100%, respectively. The former is denoted by H(10)-Z and the latter by H(100)-Z. All catalysts were sieved to 36/60 mesh powders to use for reactions, as in the previous work (11).

In the XPS measurements, only Ce^{3+} peaks were observed for Ce-Z, Ce-M, and Ce-Y, while weak Ce^{4+} peaks, in addition to Ce^{3+} , were observed for Ce/SI. The ratios of peak intensity of Ce to Si ($\text{Ce}^{3+}_{3d5/2}/\text{Si}_{2p3/2}$) were in the order of $\text{Ce-Z} \approx \text{Ce/SI} < \text{Ce-M} < \text{Ce-Y}$, and this order was not consistent with that of Ce-doping ($\text{Ce-Z} < \text{Ce-M} < \text{Ce/SI} < \text{Ce-Y}$). This fact indicates that the dispersion of Ce is lower for Ce/SI than the other catalysts. XRD patterns of Ce-Z, Ce-M, and Ce-Y showed only the peaks of the corresponding Na-zeolites, while Ce/SI had broad peaks assigned to CeO_2 . These facts indicate that Ce^{3+} ion are highly dispersed in Ce-Z, Ce-M, and Ce-Y, but Ce exists mainly in the form of CeO_2 in the case of Ce/SI.

Reactions

Three kinds of reactions were performed with a fixed-bed flow reactor as described previously (15): (i) $\text{NO} + \text{C}_3\text{H}_6 + \text{O}_2 \rightarrow \text{N}_2 + \text{CO}_x + \text{H}_2\text{O}$, (ii) $\text{NO}_2 + \text{C}_3\text{H}_6 + \text{O}_2 \rightarrow \text{N}_2 + \text{CO}_x + \text{H}_2\text{O}$, and (iii) $\text{NO} + 1/2\text{O}_2 \rightarrow \text{NO}_2$. The catalysts were pretreated at 773 K for 2 h in He. Then a mixed gas (NO or NO_2 , 1000 ppm; C_3H_6 , 500 ppm; O_2 , 2%; He, balance) was fed to the catalysts. The reaction temperature was lowered stepwise from the highest temperature after reaching steady-state at each temperature. The contact time (W/F) was changed by the catalyst weight from 0.05 to 0.5 g at a constant flow rate of $150 \text{ cm}^3 \text{ min}^{-1}$ except for the case of $W/F = 0.008 \text{ g s cm}^{-3}$ (catalyst weight (W), 0.03 g; flow rate (F), $220 \text{ cm}^3 \text{ min}^{-1}$).

Propene and NO_2 Adsorptions

Adsorptions of propene and NO_2 were carried out in the fixed-bed flow reactor. Catalyst weights used were 0.1 g for Na-Z, Na-M, and Na-Y and 0.5 g for SL and SI. Catalysts were pretreated at 773 K for 2 h in He and cooled down to room temperature (ca. 298 K). Then 500 ppm C_3H_6 or 1000 ppm NO_2 (He balance) was fed at a rate of $150 \text{ cm}^3 \text{ min}^{-1}$. After the adsorption was saturated (this adsorption amount is called the amount of total adsorption), the feed gas was then changed to pure He to replace the gas phase and reversibly desorbed species was measured (this desorption amount is called the amount of reversible adsorption). After C_3H_6 or NO_2 at the outlet reached an undetectable level, the temperature of the catalysts was raised at 5° min^{-1} to 873 K in He and desorbed species were measured as well. This desorption amount is called the amount of TPD desorption. Propene was analyzed every few minutes by GC, and NO_2 was constantly monitored by a chemiluminescence NO_x analyzer (Yanako; ELC-77A).

Analysis

The effluent gases were analyzed by a gas chromatograph (Nippon Tyran; M-200) for N_2 , CO, CO_2 , N_2O , C_2N_2 , HCN, and C_3H_6 . NO_x (NO and NO_2) were analyzed by the NO_x analyzer. The details were described in the previous paper (15).

RESULTS

$\text{NO} + \text{C}_3\text{H}_6 + \text{O}_2$ Reaction over Various Ce-Supported Catalysts

$\text{NO} + \text{C}_3\text{H}_6 + \text{O}_2$ reaction over Ce-supported catalysts was very much influenced by the kinds of catalyst carriers, as shown in Fig. 1. Among them, Ce-Z exhibited the best performance. The order of conversions of NO to N_2 (Fig. 1a) was $\text{Ce-Z} > \text{Ce-M} \gg \text{Ce-Y} > \text{Ce/SI}$, and that for C_3H_6 to CO_x was $\text{Ce-Z} > \text{Ce-M} \gg \text{Ce-Y} \approx \text{Ce/SI}$. These orders were not the same as that of the amounts of Ce doped

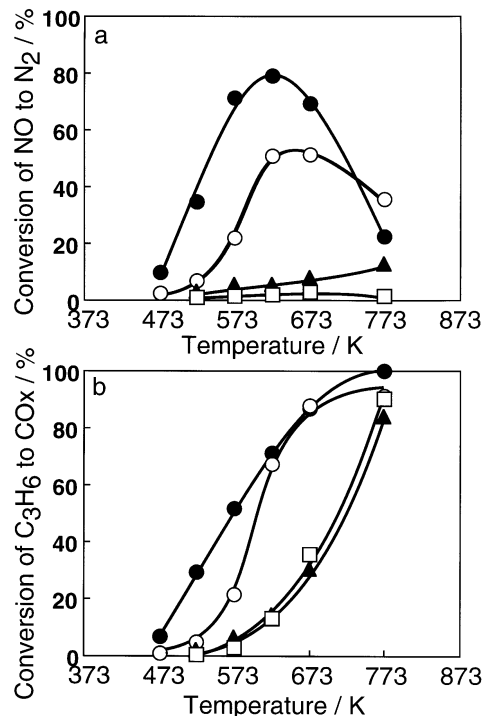


FIG. 1. Temperature dependences of (a) conversion of NO to N_2 and (b) conversion of C_3H_6 to CO_x for $\text{NO} + \text{C}_3\text{H}_6 + \text{O}_2$ reaction over Ce-supported catalysts. NO, 1000 ppm; C_3H_6 , 500 ppm; O_2 , 2%. Total flow rate, $150 \text{ cm}^3 \text{ min}^{-1}$; catalyst weight, 0.5 g ($W/F = 0.2 \text{ g s cm}^{-3}$). ●, 1.1 wt% Ce-Z; ○, 4.3 wt% Ce-M; ▲, 9.9 wt% Ce-Y; □, 5 wt% Ce/SI.

(Ce-Y (9.9 wt%) > Ce/SI (5 wt%) > Ce-M (4.3 wt%) > Ce-Z (1.1 wt%)). The order in catalytic activity becomes more remarkable, if the rates are normalized to the Ce contents. According to the XRD and XPS measurements, no cerium oxide was present, so that the dispersions of Ce would not be very different among Ce-Z, Ce-M, and Ce-Y. Hence, it is probable that the carriers themselves strongly affect the $\text{NO} + \text{C}_3\text{H}_6 + \text{O}_2$ reaction.

The rate of NO oxidation ($\text{NO} + 1/2\text{O}_2 \rightarrow \text{NO}_2$), which is the initial and indispensable step for $\text{NO} + \text{C}_3\text{H}_6 + \text{O}_2$ reaction (11, 15), was in the order of $\text{Ce-M} > \text{Ce-Z} \approx \text{Ce-Y} \approx \text{Ce/SI}$ (Fig. 2), which is much different from the relative order observed for the $\text{NO} + \text{C}_3\text{H}_6 + \text{O}_2$ reaction.

$\text{NO}_2 + \text{C}_3\text{H}_6 + \text{O}_2$ Reaction over Several Ion-Exchanged ZSM-5

Figure 3 shows the conversions of NO_2 to N_2 for $\text{NO}_2 + \text{C}_3\text{H}_6 + \text{O}_2$ reaction over Na-, Ce-, and H-exchanged ZSM-5. Ce-Z exhibited the highest conversion to N_2 . It is noteworthy that even Na-Z exhibited a significant conversion of NO_2 to N_2 , as reported in our previous paper (15). When protons were substituted for Na ions, the conversions of NO_2 to N_2 decreased with the extent of proton exchange (Na-Z > H(10)-Z > H(100)-Z). Figure 4 shows the selectivities to N-containing products at 573 K for this reaction.

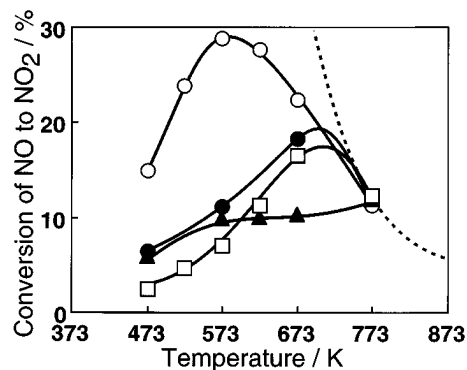


FIG. 2. Temperature dependences of conversion of NO to NO₂ for NO + 1/2O₂ → NO₂ reaction over Ce-supported catalysts. NO, 1000 ppm; O₂, 2%. Total flow rate, 150 cm³ min⁻¹; catalyst weight, 0.5 g (W/F = 0.2 g s cm⁻³). ●, 1.1 wt% Ce-Z; ○, 4.3 wt% Ce-M; ▲, 9.9 wt% Ce-Y; □, 5 wt% Ce/SI; - - -, percentage conversion at equilibrium.

Here, the selectivity is defined by

$$\% \text{Selectivity} = 100 \times (\text{number of N-containing molecules produced}) \times (\text{number of N in the molecule}) / (\text{number of NO}_2 \text{ consumed}). \quad [5]$$

No NO₂ was observed at the outlet in the whole temperature region (473–673 K) for all catalysts. That is, the conversions of NO₂ were all 100%. Therefore, the conversions to N₂ in Fig. 3 are the same as the selectivities to N₂ in Fig. 4. NO and N₂O were also formed for NO₂ + C₃H₆ + O₂ reaction. In addition, HCN was observed over Na-Z. NO was probably formed not from the dissociation of NO₂ (NO₂ → NO + 1/2O₂) but from the reaction between NO₂ and propene, because the dissociation of NO₂ was very slow for both Ce-Z and Na-Z (15). In short, NO₂ + C₃H₆ + O₂ reaction (including NO₂ to NO) was very fast over all of Na-Z, H-Z, and Ce-Z (conversions of NO₂ were all 100%), but the selectivity to N-containing products (N₂,

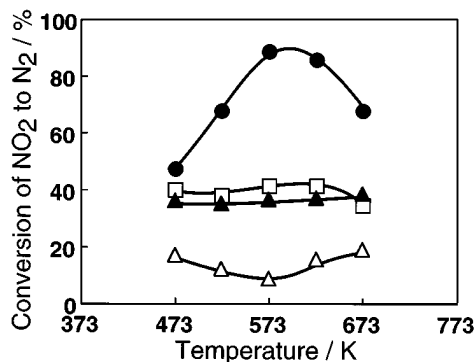


FIG. 3. Temperature dependences of conversion of NO₂ to N₂ for NO₂ + C₃H₆ + O₂ reaction over various ion-exchanged ZSM-5 catalysts. NO₂, 1000 ppm; C₃H₆, 500 ppm; O₂, 2%. Total flow rate, 150 cm³ min⁻¹; catalyst weight, 0.5 g (W/F = 0.2 g s cm⁻³). □, Na-Z; ▲, H(10%, ion-exchange level)-Z; △, H(100%)-Z; ●, Ce(19%, equal to 1.1 wt%)-Z.

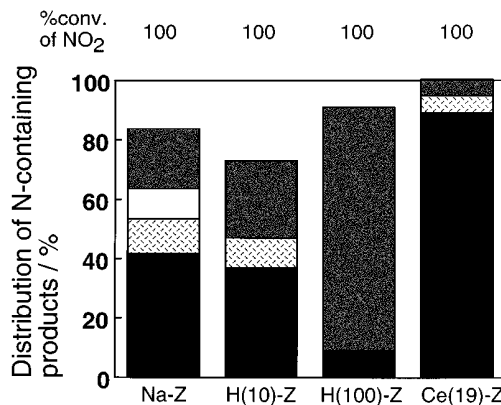


FIG. 4. Distributions of nitrogen-containing products at W/F = 0.2 g s cm⁻³ for NO₂ + C₃H₆ + O₂ reaction over various ion-exchanged ZSM-5 catalysts. Reaction temperature, 573 K. ■, N₂; ▨, N₂O; □, HCN; □, NO.

N₂O, NO, and HCN) was dependent on the kinds of cations doped.

Ce-Z and H-Z had high activities for both NO + 1/2O₂ → NO₂ and NO + C₃H₆ + O₂ reactions. Therefore, it is probable that NO formed from NO₂ + C₃H₆ + O₂ reaction was oxidized again to NO₂ on the surface and it reacted with propene to produce N₂ (Eq. [3]). Thus, the initial selectivities to N₂ directly formed from NO₂ must be smaller than those given in Fig. 4 in the cases of Ce-Z and H-Z.

On the other hand, in the case of Na-Z, since both NO + 1/2O₂ → NO₂ and NO + C₃H₆ + O₂ → N₂ reactions were very slow, N₂ was formed only directly from the NO₂ + C₃H₆ + O₂ reaction. Therefore, the data in Fig. 4 show that Na ion in zeolites has higher selectivity to direct formation of N₂ in the NO₂ + C₃H₆ + O₂ reaction than proton in zeolites. However, it is difficult to compare Na ion and Ce ion because of the reason described above, although Ce was apparently more selective.

Hence, the selectivities were compared as described below by using Na zeolites instead of Ce zeolites.

NO₂ + C₃H₆ + O₂ Reaction over Carriers Alone (Na-Zeolites, Silicalite, and SiO₂)

Figure 5 shows the temperature dependences of (a) the conversion of NO₂ to N₂ and (b) the conversion of NO₂ for NO₂ + C₃H₆ + O₂ reaction at W/F = 0.2 g s cm⁻³. The conversion to N₂ was the highest for Na-Z. N₂ was not formed at all on SI. It is noteworthy that the order of the conversion of NO₂ to N₂, i.e., Na-Z > Na-M > Na-Y > SI, was the same as that of the conversion of NO to N₂ for NO + C₃H₆ + O₂ reaction over Ce-supported catalysts (Ce-Z > Ce-M > Ce-Y > Ce/SI, Fig. 1). The conversions of NO₂ were very high in the whole temperature range for Na-Z, Na-M, and Na-Y, while it was low for SI.

Figure 6 shows the selectivities to N-containing products at 573 K. Na-Z exhibited the highest selectivity to N₂. C₂N₂ was observed on Na-M and Na-Y, in addition to N₂, N₂O,

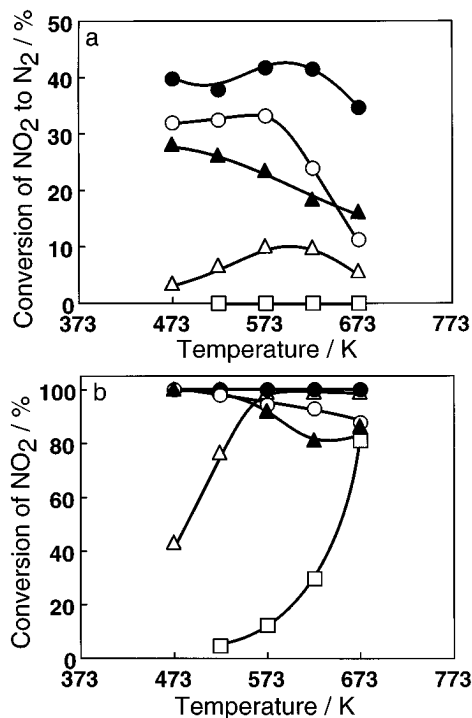


FIG. 5. Temperature dependences of (a) conversion of NO₂ to N₂ and (b) conversion of NO₂ for NO₂ + C₃H₆ + O₂ reaction over carriers (Na-zeolites, SL, and SI). NO₂, 1000 ppm; C₃H₆, 500 ppm; O₂, 2%. Total flow rate, 150 cm³ min⁻¹; catalyst weight, 0.5 g ($W/F = 0.2$ g s cm⁻³). ●, Na-Z; ○, Na-M; ▲, Na-Y; △, SL; □, SI.

and NO. C₂N₂ was also observed on Na-Z at a shorter contact time, although it was not detected at $W/F = 0.2$ g s cm⁻³. HCN was observed on Na-Z and Na-M. N₂ and NO were formed on SL, while only NO was produced on SI.

The selectivities at 623 and 673 K were not very different from those at 573 K, although the selectivities to N₂, N₂O, and C₂N₂ were slightly lower and that to NO was higher in the case of Na-zeolites and SL.

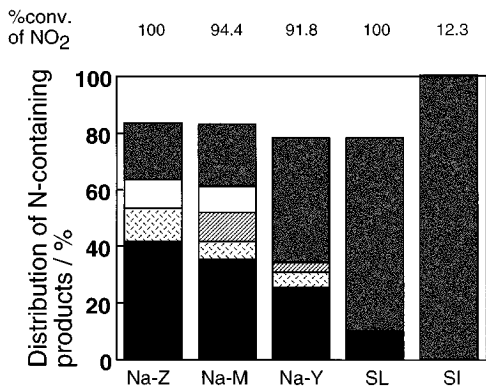


FIG. 6. Distributions of nitrogen-containing products at $W/F = 0.2$ g s cm⁻³ for NO₂ + C₃H₆ + O₂ reaction over carriers (Na-zeolites, SL, and SI). Reaction temperature, 573 K. ■, N₂; ▨, N₂O; ▩, C₂N₂; □, HCN; □, NO.

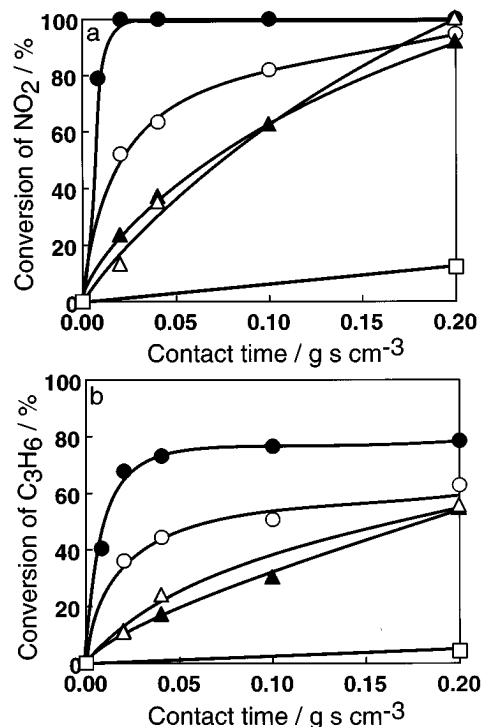


FIG. 7. Dependences of (a) conversion of NO₂ and (b) conversion of C₃H₆ on contact time at 573 K for NO₂ + C₃H₆ + O₂ reaction over carriers (Na-zeolites, SL, and SI). NO₂, 1000 ppm; C₃H₆, 500 ppm; O₂, 2%. ●, Na-Z; ○, Na-M; ▲, Na-Y; △, SL; □, SI.

Figure 7 shows the dependences of the conversions of NO₂ and C₃H₆ on contact time for NO₂ + C₃H₆ + O₂ reaction at 573 K. The conversion of NO₂ changed in close correspondence to the conversion of C₃H₆, indicating that they were consumed by the reaction with each other, that is, C₃H₆ + nNO₂ → X. Here, X is, for example, CH₂(NO₂)CH(NO₂)CH₃ and/or CH₂(NO₂)CH(ONO)CH₃. If so, the rate of reaction between NO₂ and propene can be represented by the rate of NO₂ or C₃H₆ consumed. The rate was in the order of Na-Z > Na-M > Na-Y ≈ SL > SI.

Figure 8 shows the propene utilization which is defined by the ratio of the number of O atoms in CO, CO₂, and H₂O coming from NO₂ to the number of total O atoms in CO, CO₂, and H₂O (see Appendix). In this definition, if O₂ does not contribute to the reaction, the propene utilization becomes 100%. For all catalysts, the propene utilization was high, but not 100%, which indicates that propene reacts mainly with NO₂, but only a little amount of O₂ is involved in the reaction. The oxidation of propene by O₂ in the absence of NO_x, that is, C₃H₆ + O₂ → CO_x + H₂O, was very slow on these catalysts; the conversion of C₃H₆ to CO_x was 0% on Na-Z at 573 K for the C₃H₆ (500 ppm) + O₂ (2%) reaction. Therefore, it is not likely that O₂ in the NO(NO₂) + C₃H₆ + O₂ reactions directly reacts with propene, but it probably reacts with compounds formed by the reaction between C₃H₆ and NO₂.

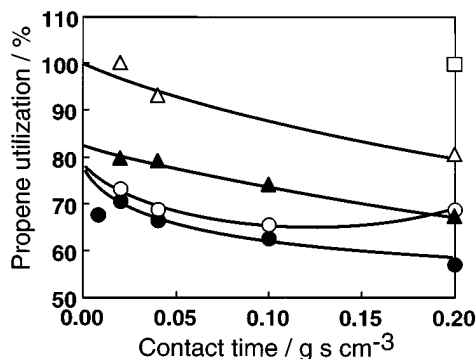


FIG. 8. Dependences of propene utilization on contact time at 573 K for $\text{NO}_2 + \text{C}_3\text{H}_6 + \text{O}_2$ reaction over carriers (Na-zeolites, SL, and SI). NO_2 , 1000 ppm; C_3H_6 , 500 ppm; O_2 , 2%. ●, Na-Z; ○, Na-M; ▲, Na-Y; △, SL; □, SI.

Figure 9 shows the dependences on contact time of the selectivities at 573 K calculated by Eq. [5]. As for Na-zeolites, with an increase in contact time the selectivity to N_2 increased and the selectivities to NO and C_2N_2 decreased. N_2O was not dependent on contact time. For SL, both the selectivity to N_2 and that to NO were independent of the contact time.

Figure 10 shows the temperature dependence of the rate of NO_2 consumption, which represents the rate of $\text{C}_3\text{H}_6 + n\text{NO}_2 \rightarrow \text{X}$ for $\text{NO}_2 + \text{C}_3\text{H}_6 + \text{O}_2$ reaction. Na-Z exhibited the highest rate. The rate decreased with an increase

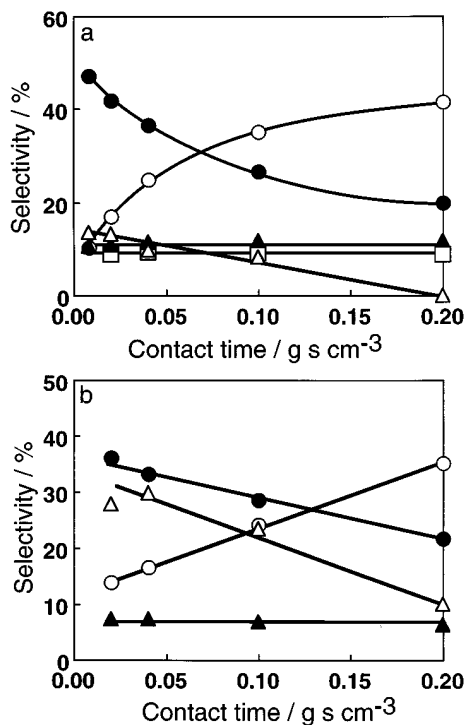


FIG. 9. Dependence of selectivities to nitrogen-containing products at 573 K for $\text{NO}_2 + \text{C}_3\text{H}_6 + \text{O}_2$ reaction over (a) Na-Z, (b) Na-M, (c) Na-Y, and (d) SL. ○, N_2 ; ▲, N_2O ; △, C_2N_2 ; □, HCN; ●, NO.

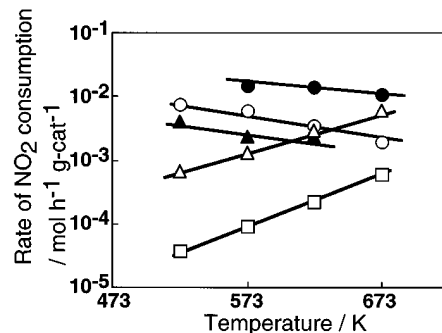


FIG. 10. Temperature dependences of the rate of NO_2 consumption for $\text{NO}_2 + \text{C}_3\text{H}_6 + \text{O}_2$ reaction over carriers (Na-zeolites, SL, and SI). NO_2 , 1000 ppm; C_3H_6 , 500 ppm; O_2 , 2%. ●, Na-Z; ○, Na-M; ▲, Na-Y; △, SL; □, SI.

in temperature for all Na-zeolites, while the rate increased with an increase in temperature for SL and SI.

C_3H_6 and NO_2 Adsorptions

The amounts of propene and NO_2 adsorbed at room temperature are summarized in Table 1. As for propene adsorption on ion-exchanged ZSM-5, Na-Z showed the smallest amount of adsorption ($\text{C}_3\text{H}_6/\text{Al} = 0.88$). Propene adsorbed was all desorbed into gas phase as propene, so that the material balance was held. The amount of propene adsorbed increased with the increment of proton

TABLE 1
Amounts of C₃H₆ or NO₂ Adsorbed at Room Temperature

Catalyst	Al(10 ⁻⁵ mol g ⁻¹)	BET(m ² /g ⁻¹)	C ₃ H ₆ uptake (10 ⁻⁵ mol g ⁻¹)				NO ₂ uptake (10 ⁻⁵ mol g ⁻¹)			
			Total ^a	Rev. ^b	TPD ^c	Bal.(%) ^d	Total ^a	Rev. ^b	TPD ^c	Bal.(%) ^d
Na-Z	122.0	326	106.9	37.7	65.3	96	178.0	85.8	97.7	96
Ce(19)-Z ^e	122.0	313	125.6	31.7	40.6	58	178.5	69.5	107.1	99
H(10)-Z ^e	122.0	—	119.5	39.2	60.6	84	157.2	68.0	92.2	100
H(100)-Z ^e	122.0	—	263.8	0	30.2	11	105.8	64.7	36.1	95
Na-M	143.4	399	50.5	29.2	21.8	98	220.2	103.3	111.6	98
Na-Y	400.2	870	39.0	37.5	2.0	100	336.0	166.8	154.0	95
Silicalite	1.6	356	12.4	11.0	0.3	91	4.2	3.2	0.9	96
SiO ₂	0	347	Trace	Trace	Trace	—	Trace	Trace	Trace	—

^a The amount of C₃H₆ or NO₂ adsorbed at 298 K under the partial pressure of 500 ppm of C₃H₆ or 1000 ppm of NO₂.

^b The amount of C₃H₆ or NO₂ desorbed in He at 298 K.

^c The amount of C₃H₆ or NO₂ desorbed during TPD in He (5° min⁻¹) up to 873 K.

^d Bal. = 100 × (Rev. + TPD)/Total.

^e Ion exchange level in parenthesis. The rests are supposedly Na.

or Ce exchanged (Na-Z < H(10)-Z < Ce(19)-Z < H(100)-Z), but the material balance became worse (Na-Z > H(10)-Z > Ce(19)-Z > H(100)-Z). Propene on H(100)-Z was not desorbed reversibly at room temperature. Figure 11 shows TPD profiles of propene adsorbed. Propene adsorbed on Na-Z was all desorbed below 473 K. With an increase in the exchange level of proton or Ce, the amounts of propene desorbed below 473 K decreased and those desorbed above 473 K increased. Propene was not desorbed at all below 473 K for H(100)-Z.

Among Na-zeolites, the amount of propene tended to increase with an decrease in the micropore size of zeolites (Na-Z(5.4 Å) > Na-M(6.7 × 7.0 Å) > Na-Y (7.4 Å) (27)), regardless of the amount of Na content. The mass balances were good for all Na-zeolites, as propene adsorbed was all desorbed below 473 K. SL, which has the same micropore structure as ZSM-5, showed much smaller amount of propene adsorbed than Na-Z. SI adsorbed little propene.

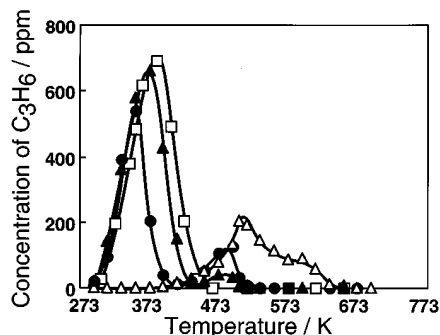


FIG. 11. TPD profiles of propene adsorbed on various ion-exchanged ZSM-5 catalysts. □, Na-Z; ▲, H(10%)⁻Z; △, H(100%)⁻Z; ●, Ce(19%)⁻Z. Adsorption, C₃H₆, 500 ppm; total flow rate, 150 cm³ min⁻¹; catalyst weight, 0.1 g. Desorption, temperature was raised at 5° min⁻¹ in He.

In the case of NO₂ adsorption on ion-exchanged ZSM-5, the amount decreased with the extent of proton exchange of Na-Z. The amount for H(100)-Z was 60% of that for Na-Z. For all catalysts, NO₂ adsorbed were all desorbed as NO₂ in TPD experiments, so that the mass balances were good. Among Na-zeolites, the amounts of NO₂ adsorbed were in parallel with the Na content (Na-Y > Na-M > Na-Z). The NO₂/Na ratio was Na-Z, 1.46; Na-M, 1.54; and Na-Y, 0.84. Taking into account that 32% of the exchange sites of Na-Y are inaccessible, being located in hexagonal prism (28), the NO₂/Na for the accessible Na is considered to be 1.24 rather than 0.84 for Na-Y. NO₂ was little adsorbed on SL and SI, both of which have very low contents of Na and Al.

When a mixture of C₃H₆ (500 ppm) and NO₂ (1000 ppm) was fed to Na-Z at room temperature, the amounts of C₃H₆ and NO₂ adsorbed were 82.1 × 10⁻⁵ mol g⁻¹ and 198.0 × 10⁻⁵ mol g⁻¹, respectively. These amounts were not very different from those in the case of the separate adsorption (C₃H₆, 106.9 × 10⁻⁵ mol g⁻¹; and NO₂, 178.0 × 10⁻⁵ mol g⁻¹, respectively). In the case of coadsorption, propene was desorbed in TPD experiment not as propene but as CO and CO₂ accompanied by the production of N₂, N₂O, and NO. One-fourth of NO₂ adsorbed was desorbed into gas phase as NO₂. The amounts of N and C recovered by TPD up to 873 K were 50 and 20%, respectively, for coadsorption.

DISCUSSION

We presumed previously that the oxidation of NO to NO₂ is the initial and indispensable step of NO + C₃H₆ + O₂ over Ce-Z (15). As for the various Ce-supported catalysts studied in the present work, however, the order of the rate of NO + C₃H₆ + O₂ → N₂, etc. (that is, Ce-Z > Ce-M ≫ Ce-Y > Ce/SI), was quite different from that of NO + 1/2O₂ → NO₂ (Ce-M > Ce-Z ≈ Ce-Y ≈ Ce/SI). This

fact indicates that the reaction between propene and NO_2 , subsequent to the oxidation of NO , is much influenced by the kinds of carriers. This must be because (i) the property of Ce ion itself such as valence and coordination number and/or (ii) the surroundings of Ce ion (or "reaction field") much change depending on the carriers.

It is noteworthy that both the order of the rate of $\text{C}_3\text{H}_6 + n\text{NO}_2 \rightarrow \text{X}$ and that of the selectivity to N_2 for $\text{NO}_2 + \text{C}_3\text{H}_6 + \text{O}_2$ reaction over the carriers ($\text{Na-Z} > \text{Na-M} > \text{Na-Y} > \text{SI}$) agreed with the order of the rate of N_2 formation for $\text{NO} + \text{C}_3\text{H}_6 + \text{O}_2$ reaction over Ce-supported catalysts ($\text{Ce-Z} > \text{Ce-M} > \text{Ce-Y} > \text{Ce/SI}$). This agreement is understandable if one considers that NO is oxidized to NO_2 over Ce-sites and assumes that the subsequent reaction between propene and NO_2 is similar between Ce-zeolites and Na-zeolites. In other words, if NO is once oxidized to NO_2 , Na- and Ce-zeolites behave very similarly. Since Ce ion must be much different from Na ion in such properties as valence, coordination, and redox property, it is rather natural to assume that the similarity is caused by the zeolite structure itself, that is, the surroundings of the metal ions. This property is presumably crucial for the reaction between propene and NO_2 , as discussed below.

First, we discuss the relation between the rate and selectivity of $\text{NO}_2 + \text{C}_3\text{H}_6 + \text{O}_2$ reaction and the surroundings of metal ion in the case of Na-zeolites. Then, on this basis, we speculate the relation between the surroundings of Ce ion and the reaction between propene and NO_2 .

The influences of the kinds of carriers on $\text{NO} + \text{hydrocarbons} + \text{O}_2$ reactions have been indicated in the literature. Iwamoto *et al.* reported that the conversion of NO to N_2 for $\text{NO} + \text{C}_2\text{H}_4 + \text{O}_2$ reaction decreased as $\text{Cu-ZSM-5} > \text{Cu-mordenite} > \text{Cu-L zeolite} > \text{Cu-ferrierite}$ (24). According to Kikuchi *et al.* the conversion of NO to N_2 for $\text{NO} + \text{CH}_4 + \text{O}_2$ reaction is in the order of $\text{H-ZSM-5} > \text{H-mordenite} > \text{H-ferrierite} > \text{H-USY}$ (ultra-stable Y zeolite) and the ratio of NO reacted to CH_4 consumed is in the order of $\text{H-ferrierite} > \text{H-mordenite} > \text{H-ZSM-5} > \text{H-USY}$, the latter order being in accordance with that of the acid strength of zeolite (25). Li and Armor observed that the order of the conversion of NO to N_2 was $\text{Co-ferrierite} > \text{Co-ZSM-5} > \text{Co-mordenite} > \text{Co-L} > \text{Co-Y}$ for the $\text{NO} + \text{CH}_4 + \text{O}_2$ reaction, which corresponded to the amount of NO adsorbed per Co ion; Co-ZSM-5 ($\text{NO}/\text{Co} = 1.1$) $>$ Co-mordenite ($\text{NO}/\text{Co} = 0.8$) $>$ Co-Y ($\text{NO}/\text{Co} = 0.06$) (26). They have indicated that the electronic influence of the cations in the zeolite framework is important. Thus, the influences of carriers are remarkable, but still need to be elucidated.

$\text{NO}_2 + \text{C}_3\text{H}_6 + \text{O}_2$ Reaction over Na-Zeolite, Silicalite, and SiO_2 (Carriers)

1. Active site for the reaction and adsorption. As shown in Figs. 3 and 4, the selectivity to N_2 for $\text{NO}_2 + \text{C}_3\text{H}_6 + \text{O}_2$

reaction decreased with the extent of proton exchange of Na-Z. Na-Z has little protonic acidity as discussed below and the rate of $\text{NO}_2 + \text{C}_3\text{H}_6 + \text{O}_2$ reaction was much faster on Na-Z than on SL (Fig. 11). These facts suggest that Na ion is the active site for $\text{NO}_2 + \text{C}_3\text{H}_6 + \text{O}_2$ reaction over Na-Z. However, this is apparently contrary to the result for the $\text{NO}_2 + \text{CH}_4$ or the $\text{NO} + \text{CH}_4 + \text{O}_2$ reaction in which Na-Z showed much lower conversion to N_2 than H-Z (29). The difference is probably due to the difference in reactivity with NO_2 between methane and propene. In the case of methane, the activation of methane may be prerequisite for the reaction with NO_2 , while NO_2 can directly react with the double-bond of propene.

Na-Z exhibited the highest rate for $\text{NO}_2 + \text{C}_2\text{H}_6 + \text{O}_2$ reaction among Na-zeolites, in spite of the lowest Na content. This fact again indicates that the environment of Na ion is important for this reaction.

In order to investigate more closely the active site, the rates of $\text{NO}_2 + \text{C}_3\text{H}_6 + \text{O}_2$ reaction (mainly, $\text{C}_3\text{H}_6 + n\text{NO}_2 \rightarrow \text{X}$) in Fig. 7 and the amounts of propene or NO_2 adsorbed at room temperature (Table 1) are compared in Fig. 12. The rate of $\text{NO}_2 + \text{C}_3\text{H}_6 + \text{O}_2$ reaction is approximately proportional to the amount of C_3H_6 adsorbed (Fig. 12a) and is little correlated to the amount of NO_2

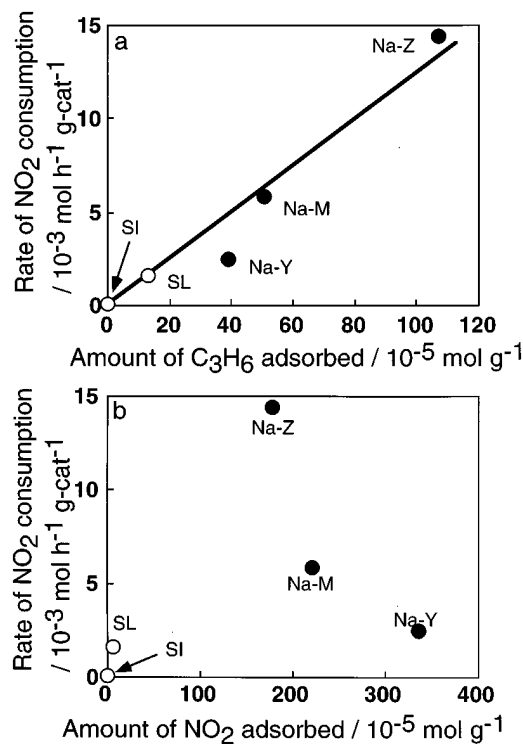


FIG. 12. (a) Relationship between the rate of NO_2 consumption for $\text{NO}_2 + \text{C}_3\text{H}_6 + \text{O}_2$ reaction (Fig. 11) and the amounts of propene adsorbed (Table 1) and (b) that between the rates of NO_2 reacted for $\text{NO}_2 + \text{C}_3\text{H}_6 + \text{O}_2$ reaction and the amounts of NO_2 adsorbed (Table 1) over carriers (Na-zeolites, SL, and SI).

adsorbed (Fig. 12b). The correlation in Fig. 12a indicates that the site for propene adsorption is the active site for $\text{NO}_2 + \text{C}_3\text{H}_6 + \text{O}_2$ reaction.

Next, we discuss the site for propene adsorption. The amount of propene adsorbed on Na-Z was much larger than that on SL, although they have the same microstructure. Propene adsorbed on Na-Z was all desorbed as propene into gas phase below 473 K and the mass balance was quite good. On the other hand, for H(10)-Z, H(100)-Z, and Ce(19)-Z, the balances became worse with an increase in proton or Ce exchange of Na-Z, and propene was desorbed above 473 K. This shows that Na-Z has little protonic acidity and adsorbs propene intact on Na ion. In the case of H(10)-, H(100)-, and Ce(19)-Z, propene probably reacts at protonic acid sites to form oligomers. This explanation is supported by the report that 1-butene is adsorbed as it is on Na ion of Na-Y, while it reacts on a protonic acid site to form oligomer species on NaH-Y (30).

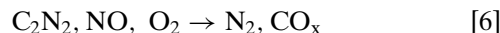
Na-M and Na-Y held smaller amounts of propene than Na-Z, inspite of the greater Na content ($\text{C}_3\text{H}_6/\text{Na}$ ratio: Na-Z, 0.88; Na-M, 0.35; Na-Y, 0.14). Here, the amount of inaccessible Na ion in hexagonal prism (28) was subtracted for Na-Y, as described above. In the cases of Na-M and Na-Y, propene was all desorbed below 473 K and the balance was as good as Na-Z, indicating that Na-M and Na-Y also have little protonic acidity and adsorb propene on Na ion. However, the ratio of propene adsorbed to Na ion was larger for zeolites having smaller micropores (Na-Z (5.4 Å) > Na-M (6.7 × 7.0 Å) > Na-Y (7.4 Å)). This implies that the stabilization in micropore (e. g., van der Waals interaction between the surface of micropore and propene) must be considered for the adsorption of propene.

On the other hand, the adsorption of NO_2 on Na-zeolites appeared to be closely related to the Na content, regardless of the micropore size. The NO_2/Na ratio was Na-Z, 1.46; Na-M, 1.54; and Na-Y, 1.24. NO_2 adsorbed on H(100)-Z was 60% of Na-Z. SL and SI, both of which contained little Na and Al, held little NO_2 . Hence, it is considered that NO_2 is adsorbed on Na ion in the case of Na-zeolites and the surroundings of Na ion do not much affect the adsorption of NO_2 . Present results are comparable with those in the literature. Recently, Adelman *et al.* reported that two NO_2 per Na ion were adsorbed over Na-ZSM-5 (31).

On the basis of these results, it may be proposed that the active site of Na-zeolites for $\text{NO}_2 + \text{C}_3\text{H}_6 + \text{O}_2$ reaction is Na ion on which propene can be adsorbed. The number of site is Na-Z; $106.9 \times 10^{-5} \text{ mol g}^{-1}$, Na-M; $50.5 \times 10^{-5} \text{ mol g}^{-1}$, and Na-Y; $39.0 \times 10^{-5} \text{ mol g}^{-1}$. Hereafter, these Na ions are denoted by Na(A), and the rest by Na(B). The fraction of Na(A), namely $\text{Na(A)} / \{\text{Na(A)} + \text{Na(B)}\}$, was 0.88 for Na-Z, 0.35 for Na-M, and 0.14 for Na-Y.

2. Secondary reactions Na-Z exhibited the highest selectivity to N_2 at $W/F = 0.2 \text{ g s cm}^{-3}$ for $\text{NO}_2 + \text{C}_3\text{H}_6 + \text{O}_2$ reaction, as shown in Fig. 6. However, the selectivities to

N_2 increased with contact time for Na-zeolites, indicating that N_2 is formed not only as a primary product but also as a product of secondary reaction. On these catalysts, since both $\text{NO} + 1/2\text{O}_2 \rightarrow \text{NO}_2$ and $\text{NO} + \text{C}_3\text{H}_6 + \text{O}_2 \rightarrow \text{N}_2$ were very slow, the secondary reaction is probably not the $\text{NO} + \text{C}_3\text{H}_6 + \text{O}_2$ reaction. If one considers that both the selectivity to C_2N_2 and that to NO decreased with contact time and that the selectivities to N_2 and NO were little dependent on the contact time for SL on which C_2N_2 was not formed, the secondary reaction to form N_2 is possibly the reaction between NO and C_2N_2 (Eq. [6]). It is suggested that O_2 is also involved in the secondary reaction, since the propene utilization for $\text{NO}_2 + \text{C}_3\text{H}_6 + \text{O}_2$ reaction decreased with the increase in contact time:



The selectivity to N_2O were always independent of the contact time, indicating that N_2O is formed only as a primary product and is not involved in the secondary reaction.

Figure 13 shows the initial selectivities extrapolated to $W/F = 0 \text{ g s cm}^{-3}$ using the data in Fig. 9. As for Na-zeolites, although the selectivities at $W/F = 0.2 \text{ g s cm}^{-3}$ (Fig. 6) were different, the initial ones were more or less similar. That is, the reason why selectivity to N_2 at $W/F = 0.2 \text{ g s cm}^{-3}$ was highest for Na-Z is probably that the $\text{NO}_2 + \text{C}_3\text{H}_6 + \text{O}_2$ reaction was fastest and the secondary reaction (Eq. [6]) proceeded to the deepest extent. Actually, C_2N_2 already disappeared at $W/F = 0.2 \text{ g s cm}^{-3}$ only for Na-Z. On the other hand, C_2N_2 was not formed and the selectivities to N_2 and NO did not depend on contact time over SL. Only NO was produced on SI. On the basis of the differences in the selectivities as primary products for $\text{NO}_2 + \text{C}_3\text{H}_6 + \text{O}_2$ reaction, catalysts can be divided into three groups: Na-zeolites, SL, and SI.

3. Coadsorption of NO_2 and propene: As discussed earlier, in the case of Na-zeolites, Na ion (Na(A)) on which propene can be adsorbed is considered to be the active site

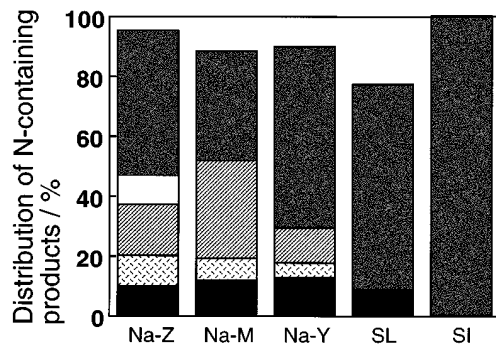


FIG. 13. Distributions of nitrogen-containing products at $W/F = 0 \text{ g s cm}^{-3}$, obtained from Fig. 10, for $\text{NO}_2 + \text{C}_3\text{H}_6 + \text{O}_2$ reaction over carriers (Na-zeolites, SL, and SI). Reaction temperature, 573 K. ■, N_2 ; □, N_2O ; ▨, C_2N_2 ; ▩, NO.

for $\text{NO}_2 + \text{C}_3\text{H}_6 + \text{O}_2$ reaction. NO_2 was adsorbed on almost all Na ion ($\text{Na(A)} + \text{Na(B)}$), regardless of the kinds of zeolites. Therefore, it is presumable that Na(A) can adsorb both propene and NO_2 . Here, there evolves a question whether or not both propene and NO_2 can be adsorbed simultaneously on Na(A) during $\text{NO}_2 + \text{C}_3\text{H}_6 + \text{O}_2$ reaction. According to the results of coadsorption of propene and NO_2 at room temperature, the amounts of propene and NO_2 adsorbed were similar to those in the case of the separate adsorption. However, during TPD in He after the coadsorption propene was not desorbed at all and the amount of NO_2 desorbed was significantly smaller than that adsorbed. According to IR study, the bands assigned to organic nitro and nitrite compounds were observed for Na-Z at room temperature in an $\text{NO}_2 + \text{C}_3\text{H}_6 + \text{O}_2$ mixture (32). These facts indicate that propene and NO_2 do not inhibit each other in the adsorption on Na(A) and that they are coadsorbed on the same Na ion and subsequently react to form organic nitro and nitrite compounds.

In contrast, in the case of SL, the amount of NO_2 adsorbed was much smaller than that of propene adsorbed. SI did not adsorb either propene or NO_2 at room temperature. These differences in the active sites for adsorption are probably the main reason for the different selectivities for $\text{NO}_2 + \text{C}_3\text{H}_6 + \text{O}_2$ reaction among Na-zeolites, SL, and SI, as shown in Fig. 13.

NO + C₃H₆ + O₂ Reaction over Ce-Supported Catalysts

The remarkable influences of carriers observed for $\text{NO} + \text{C}_3\text{H}_6 + \text{O}_2$ reaction catalyzed by Ce zeolites (Fig. 1) may be explained by the information obtained in the present work from $\text{NO}_2 + \text{C}_3\text{H}_6 + \text{O}_2$ reaction over Na-zeolites, as described below.

In the case of $\text{NO} + \text{C}_3\text{H}_6 + \text{O}_2$ reaction over Ce-Z, NO is oxidized to NO_2 on Ce ion and the desorption of $\text{NO}_2(\text{ad})$ is so slow that it rather desorbs by reacting with propene on Ce. This conclusion was derived from the fact that the conversion of NO to N_2 for $\text{NO} + \text{C}_3\text{H}_6 + \text{O}_2 \rightarrow \text{N}_2$ was significantly faster than the reaction in the steady state of $\text{NO} + 1/2\text{O}_2 \rightarrow \text{NO}_2$ over Ce-Z, whereas a large amount of NO_2 was adsorbed under these conditions (15). It was also reported that adsorbed NO_2 reacts with adsorbed hydrocarbon in the case of $\text{NO} + \text{hydrocarbons} + \text{O}_2$ reaction over Cu-ZSM-5 and Cu-ZrO₂, because N_2 production is slower than or equal to NO oxidation to NO_2 in the absence of hydrocarbon (33).

According to XPS and XRD measurements, it is presumed that most Ce ions exist at ion-exchange sites as Ce^{3+} ions, although the possibility that Ce ions exist in the form of ultrafine Ce_2O_3 particles in micropores cannot be excluded. If Ce ions exist at the ion-exchange sites, some Ce ions are exchanged for Na(A) which is the active site of Na zeolites for $\text{NO}_2 + \text{C}_3\text{H}_6 + \text{O}_2$ reaction and some for little active Na(B) . These two kinds of Ce ions may be denoted

by Ce(A) and Ce(B), respectively. Since Ce(A) must have the surroundings similar to Na(A) , Ce(A) possibly adsorbs both propene and NO_2 , whereas Ce(B) adsorb only NO_2 , corresponding to the difference between Na(A) and Na(B) . It is also likely, therefore, for $\text{NO} + \text{C}_3\text{H}_6 + \text{O}_2$ over Ce-zeolites that $\text{NO}_2(\text{ad})$ is formed on Ce(A) and it reacts with propene to form N_2 . In other words, the conversions to N_2 for $\text{NO} + \text{C}_3\text{H}_6 + \text{O}_2$ over Ce-zeolite are possibly determined by the amount of Ce(A). Since the amounts of Na(A) are in the order of $\text{Na-Z} > \text{Na-M} > \text{Na-Y}$, the amount of Ce(A) may be also in the order of $\text{Ce-Z} > \text{Ce-M} > \text{Ce-Y}$. This would explain the observed fact that Ce-M and Ce-Y exhibited the lower conversions to N_2 than Ce-Z in spite of the larger amount of Ce.

CONCLUSION

The reduction of NO in the $\text{NO} + \text{C}_3\text{H}_6 + \text{O}_2$ reaction over various Ce-supported catalysts was very much dependent on the kinds of catalyst carriers ($\text{Ce-ZSM-5} > \text{Ce-mordenite} \gg \text{Ce-Y zeolite} > \text{Ce/SiO}_2$). The rate of this reaction showed the same order as the rates of reduction of NO_2 for $\text{NO}_2 + \text{C}_3\text{H}_6 + \text{O}_2$ reaction over the carriers alone ($\text{Na-ZSM-5} > \text{Na-mordenite} > \text{Na-Y zeolite} > \text{SiO}_2$). Based on these results, it was concluded that the carriers play a crucial role in the formation of N_2 in the reaction between propene and NO_2 , which is the step subsequent to the oxidation of NO to NO_2 . Furthermore, as for the carriers alone the rate of $\text{NO}_2 + \text{C}_3\text{H}_6 + \text{O}_2$ reaction was in proportion to the amount of propene adsorbed at room temperature, and the amount of propene adsorbed per Na ion was larger for zeolites having smaller micropores. On the other hand, the amount of NO_2 adsorbed which was greater and comparable with the Na content was little correlated to the rates of $\text{NO}_2 + \text{C}_3\text{H}_6 + \text{O}_2$ reaction. These facts indicated that the active site on Na-zeolites for this reaction is the Na ion which can adsorb propene and that the stabilization in micropore enhances the adsorption of propene. It was further speculated that Ce ions introduced in these sites are the active sites for the $\text{NO} + \text{C}_3\text{H}_6 + \text{O}_2$ reaction over Ce-zeolite.

APPENDIX: CALCULATION OF PROPENE UTILIZATION

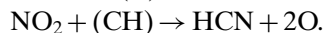
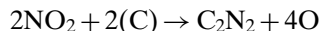
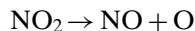
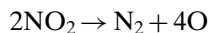
Propene utilization for $\text{NO}_2 + \text{C}_3\text{H}_6 + \text{O}_2$ reaction is defined by

$$\text{Propene utilization} = 100 \times ((a) \text{ number of oxygen atoms in CO, CO}_2, \text{ and H}_2\text{O formed coming from NO}_2) / ((b) \text{ number of total oxygen atoms in CO, CO}_2, \text{ and H}_2\text{O formed}). \quad [7]$$

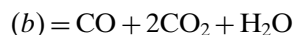
(a) is calculated by the next equation. The terms in the right-hand side of the equation are experimentally measured.



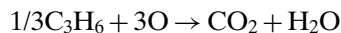
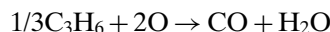
This is based on the following stoichiometries:



(b) is calculated by



H₂O is estimated based on the following stoichiometries:



ACKNOWLEDGMENT

This study was supported in part by a Grant-in-Aid for Scientific Research from the Ministry of Education, Science and Culture of Japan.

REFERENCES

- Ger. Offen DE 3642018 (1987) (Volkswagen); Japan Kokai 1988-100919 (Toyota).
- Iwamoto, M., Symposium on Catalytic Technology for the Removal of Nitrogen Oxides, pp. 17-22. Catalysis Society of Japan, 1990.
- Held, W., König, A., Richter, T., and Puppe, L., *SAE Paper* 900469 (1990).
- Hamada, H., Kintaichi, Y., Sasaki, M., and Ito, T., *Appl. Catal.* **64**, L1 (1990).
- Hamada, H., Kintaichi, Y., Sasaki, M., Ito, T., and Tabata, M., *Appl. Catal.* **70**, L15 (1991).
- Yogo, K., Tanaka, S., Ihara, M., Hishiki, T., and Kikuchi, K., *Chem. Lett.* 1025 (1992).
- Li, Y., and Armor, J. N., *Appl. Catal. B* **1**, L31 (1992).
- Inui, T., Iwamoto, S., Kojo, S., and Yoshida, T., *Catal. Lett.* **13**, 87 (1992).
- Misono, M., and Kondo, K., *Chem. Lett.* 1001 (1991).
- Yokoyama, C. and Misono, M., *Chem. Lett.* 1669 (1992).
- Yokoyama, C., and Misono, M., *Bull. Chem. Soc. Jpn.* **67**, 557 (1994).
- Sasaki, M., Hamada, H., Kintaichi, Y., and Ito, T., *Catal. Lett.* **15**, 297 (1992).
- Petunchi, J. O., and Hall, W. K., *Appl. Catal. B* **2**, L17 (1993).
- Yahiro, H., Yu-u, Y., Takeda, H., Mizuno, N., and Iwamoto, M., *Shokubai* **35**, 126 (1993).
- Yokoyama, C., and Misono, M., *J. Catal.* **150**, 9 (1994).
- Yokoyama, C., and Misono, M., *Catal. Today* **22**, 59 (1994).
- Lukyanov, D. B., Sill, G., d'Itri, J. L., and Hall, W. K., *J. Catal.* **153**, 265 (1995).
- Radtke, F., Koepfel, R. A., and Baiker, A., *Appl. Catal. A* **107**, L125 (1994).
- Radtke, F., Koepfel, R. A., and Baiker, A., *J. Chem. Soc., Chem. Commun.* **1995**, 427.
- Yokoyama, C., Yasuda, H., and Misono, M., *Shokubai* **35**, 122 (1993).
- Yasuda, H., Miyamoto, T., and Misono, M., *ACS Symposium Series No. 587*, 110 (1995).
- Tanaka, T., Okuhara, T., and Misono, M., *Appl. Catal. B* **4**, L1 (1994).
- Yokoyama, C., and Misono, M., *Catal. Lett.*, **29**, 1 (1994).
- Sato, S., Yu-u, Y., Yahiro, H., Mizuno, N., and Iwamoto, M., *Appl. Catal.* **70**, L1 (1991).
- Yogo, K., Umeno, M., Watanabe, H., and Kikuchi, E., *Catal. Lett.* **19**, 131 (1993).
- Li, Y. and Armor, J. N., *Appl. Catal. B* **2**, 239 (1993).
- Meier, W. M., and Olson, D. H., "Atlas of Zeolite Structure Types," Polycrystal Book Service, Pittsburgh, PA, 1978.
- Sherry, H. S., *J. Phys. Chem.* **70**, 1158 (1966).
- Nishizaka, Y., and Misono, M., *Chem. Lett.* 1295 (1993); 2237 (1994).
- Datka, J., *J. Chem. Soc., Faraday I* **76**, 2437 (1980).
- Adelman, B. J., Lei, G. D., and Sachtler, W. M.H., *Catal. Lett.* **28**, 119 (1994).
- Yasuda, H., Miyamoto, T., and Misono, M., unpublished results.
- Bethke, K. A., Li, C., Kung, M. C., Yang, B., and Kung, H. H., *Catal. Lett.* **31**, 287 (1995).